

IN SITU VISIBLE TO NEAR-INFRARED (VNIR) PHOTOMETRIC SPECTRAL OBSERVATIONS OF THE LUNAR REGOLITH BY CHANG'E-4. Yazhou Yang¹, Honglei Lin², Yang Liu¹, Yangting Lin², Yong Wei², Sen Hu², Wei Yang², Rui Xu³, Zhiping He³, Yongliao Zou¹. ¹National Space Science Center, CAS, Beijing 100190, China; ²Institute of Geology and Geophysics, CAS, Beijing 100029, China; ³Shanghai Institute of Technical Physics, CAS, Shanghai, 200083, China. (email: yangyazhou@nssc.ac.cn)

Introduction: VNIR reflectance spectroscopy is very useful in characterizing the surface mineralogical compositions of airless bodies. However, numerous previous studies have shown that viewing and scattering geometries may change the spectral features, including band center, band depth, and spectral slope, and thus complicate the composition interpretation [1,2]. Furthermore, the variation in phase angles may result in a reddening trend in the reflectance spectra[1]. This phase reddening effect could be coupled with the reddening effect of space weathering and mislead the interpretation of the weathering degree of the surface material.

The Hapke model is widely used in estimating mineralogical information from reflectance spectra. The simplified version of the model contains three important parameters including the single scattering albedo (SSA) and the two phase function parameters (b & c). The SSA, defined as the ratio of scattering efficiency to the sum of scattering and absorption efficiencies, is an important parameter in quantitative spectral analysis. According to Hapke, the SSA of a mixture can be taken as the linear combination of each endmember's SSA, which allows the retrieval of mineral abundances using spectral unmixing technique [3]. In theory, SSA should be independent of viewing and scattering geometries, as it is only dependent on optical constants and grain size. However, in remote sensing analysis, the SSA of a mixture cannot be directly calculated, because the optical constants and grain size of the mixture cannot easily be obtained. Instead, SSA of the mixture for lunar regolith can be derived from Hapke model by assuming known phase function parameters[3]. Alternatively, SSA and phase function parameters can be solved simultaneously through photometric measurements[4]. Proper phase function parameters are important for the accuracy of derived SSA, which is the key to reduce the uncertainty of spectral unmixing results. The effects of phase function on the derived SSA of typical lunar-type minerals have been studied in detail in [5]. The scattering properties of the lunar regolith for the whole VNIR wavelength ranges are not well understood yet, especially for the undisturbed lunar surface.

The Chang'E-4 (CE-4) has successfully landed on the far side of the Moon on January 3, 2019, and its Yutu-2 rover has explored the lunar surface for more

than 10 lunar days. The Visible and Near-infrared Imaging Spectrometer (VNIS) on board the rover provides us an excellent opportunity to study the spectral features of the lunar surface through *in situ* measurements. On the 10th lunar day of the mission operations, the VNIS carried out photometric spectral measurements at two sites along the traverse, respectively. During the measurements at each site, the position of the rover was kept unchanged and the spectra were collected at different time of the day with fixed emission angle at $\sim 45^\circ$. Since the azimuth and altitude of the sun changed with time, a series of VNIR spectra over the same area with different viewing geometries were obtained.

With these *in situ* photometric spectral data, we analyzed the effects of measurement geometries on the regolith spectral features, and evaluated the uncertainty of derived SSA, and derived the phase function parameters which characterize the surface scattering properties.

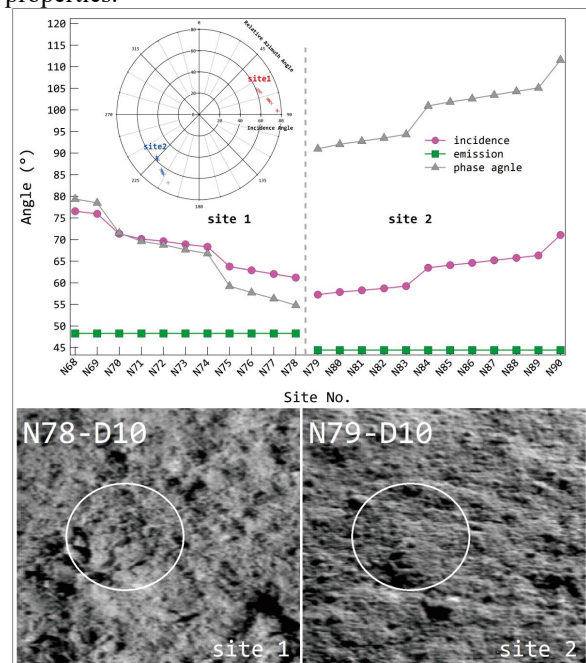


Fig. 1. Top: The incidence, emission, phase, and relative azimuth angles of the measurements; Bottom: CMOS images at 560 nm of site 1 and site 2.

Data & Method: On the 10th lunar day of mission operations, the rover firstly collected 11 spectra (ID:

N68-N78) over the exactly same area at site 1 and collected another 12 spectra (N79-N90) over site 2 (Fig. 1) which is adjacent to site 1. The angles of these measurements are shown in Fig. 1. The minimum and maximum phase angles involved in the measurements are 91 and 112 degrees, respectively. Details on the VNIS instrument can be found in [6]. The radiometric calibrated radiance data was converted to reflectance factor using the solar irradiance calibration method [7-9]. Fig. 2 shows the absolute reflectance spectra obtained at site 1 and site 2.

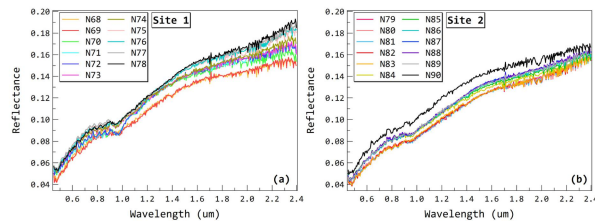


Fig. 2. Reflectance spectra obtained by Yutu-2 rover on its 10th lunar day at (a) site 1 and (b) site 2. (c) Reflectance spectra of N78 before and after smoothing; (d) Continuum-removed spectrum of N78.

The CE-4 spectra were firstly smoothed and then a straight-line segments method was employed to obtain the continuum-removed spectra. For characterizing the band center and band depth, we used a polynomial function fitting to the absorption regions around 1 μm and 2 μm . To derive the SSA and phase function parameters, we employed the same simplified Hapke model as that used in [5] and the two-term Legendre polynomial form of phase function [5]. There two parameters (b and c) in this phase function, where the parameter b describes the degree of forward/backward scattering, a negative b value means more forward scattering.

Results: As shown in Fig. 3a, the spectral slopes, defined as the ratio of reflectance at 1.7 and 0.7 μm , increase with increasing phase angles, suggesting a clear phase reddening trend. For typical lunar-type space weathering, with the increase of maturity, the spectral reddening and darkening happened simultaneously. As shown in Fig. 3b, compared to the returned lunar soil samples from the LSCC database, the CE-4 spectra show large spectral slope and low albedo values, indicating that the regolith at the measurement site is relatively mature.

Fig. 4a shows the SSAs derived with known phase function parameters ($b=-0.4$, $c=0.25$) as proposed in [10] for each CE-4 measurement. These SSAs show great variations with measurement angles, which is contradict to the fact that SSA should be independent of viewing geometry. The SSA and phase function

parameters derived from photometric fitting are shown in Fig.4. The derived b values for all wavelengths are all smaller than zero, indicating that the measured regolith is more forward scattering, similar to those silicate (olivine, pyroxene, and plagioclase) minerals.

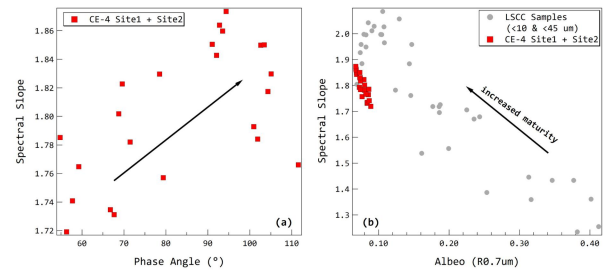


Fig. 3. (a) Spectral slopes ($R_{1.7}/R_{0.7}$) vs phase angles for the CE-4 spectra; (b) Spectral slopes vs albedo ($R_{0.7}$) for the CE-4 spectra and spectra of returned lunar soil samples with particles size $<10 \mu\text{m}$ and $<45 \mu\text{m}$ from the LSCC database.

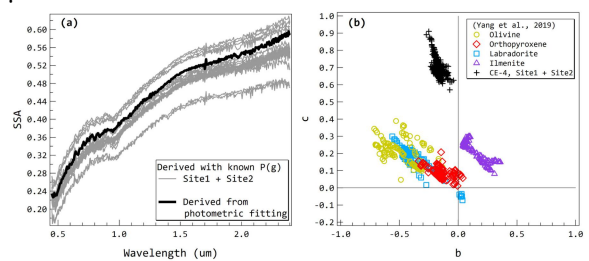


Fig. 4. (a) SSA derived from photometric fitting using the Hapke model and those derived with known phase function parameters. (b) The Legendre polynomial phase function parameters b , c for different wavelengths (0.45 - 2.395 μm) derived by fitting the photometric spectral data. The b , c values of olivine, orthopyroxene, labradorite, and ilmenite obtained by [5] are shown for comparison.

Conclusion: The spectral reddening and darkening changes caused by viewing and scattering geometries may be coupled with the effects of space weathering, which may mislead the evaluation of the lunar regolith maturity. Proper photometric correction is needed for estimating the spectral maturity. The SSA and phase function parameter values derived from photometric fitting can be used as ground-truth values for the spectral analysis of the CE-4 landing site.

References: [1] Sanchez J. A. et al. (2012) *Icarus*, 220(1). [2] Ruesch O. et al. (2015) *Icarus*, 258, 384-401. [3] Hapke B. (2012) *Cambridge University Press*. [4] Mustard J. F. et al. (1989) *JGR*, 94, 13619-13634. [5] Yang et al. (2019) *JGR*, 124. [6] Li C. et al. (2019) *Sensors*, 19(12), 2806. [7] Hu et al. (2019) *GRL* 46. [8] Zhang H. et al. (2015) *GRL*, 42(17). [9] Lin H. et al. (2019) *NSR*. [10] Lucey P. (1998) *JGR* 103(E1), 1703-1713.